ABSTRACT

MATRIX CONTINUED FRACTION APPROACH TO THE RELATIVISTIC QUANTUM MECHANICAL SPIN-ZERO FESHBACH-VILLARS EQUATIONS

By

Natalie Brown

August 2015

In this thesis we solve the Feshbach-Villars equations for spin-zero particles through use of matrix continued fractions. The Feshbach-Villars equations are derived from the Klein-Gordon equation and admit, for the Coulomb potential on an appropriate basis, a Hamiltonian form that has infinite symmetric band-matrix structure. The corresponding representation of the Green's operator of such a matrix can be given as a matrix continued fraction. Furthermore, we propose a finite dimensional representation for the potential operator such that it retains some information about the whole Hilbert space. Combining these two techniques, we are able to solve relativistic quantum mechanical problems of a spin-zero particle in a Coulomb-like potential with a high level of accuracy.

MATRIX CONTINUED FRACTION APPROACH TO THE RELATIVISTIC QUANTUM MECHANICAL SPIN-ZERO FESHBACH-VILLARS EQUATIONS

A THESIS

Presented to the Department of Physics and Astronomy

California State University, Long Beach

In Partial Fulfillment

of the Requirements for the Degree

Master of Science in Physics

Committee Members:

Zoltán Papp, Ph.D. (Chair)
Prashanth Jaikumar, Ph.D.
Jiyeong Gu, Ph.D.

College Designee:

Chuhee Kwon, Ph.D.

By Natalie Brown

B.S., Mathematics and Physics, 2010, University of Missouri, Columbia

August 2015

ProQuest LLC.
789 East Eisenhower Parkway
P.O. Box 1346
Ann Arbor, MI 48106 - 1346

ACKNOWLEDGEMENTS

I am grateful to my family, who have always supported all of my life endeavors. My parents, Ray and Tamra, taught me you can do anything want, if you just work hard. My siblings, Alysha and Ray, have constantly encouraged and believed in me. I would not be the person I am today without their love and support.

I am also thankful to my amazing group of friends who love me for the nerd that I am. They always allowed me to be myself and encouraged my scientific work.

I would like to acknowledge my CSULB physics family who helped me grow as a scientist. With their help, my abilities have been greatly strengthened and expanded.

And most importantly, I would like to thank my thesis advisor Dr. Zoltán Papp who taught me not only what makes good research, but also what makes a great scientist. He has made a great impact on my life as a teacher, mentor and scientist.

TABLE OF CONTENTS

Page

CHAPTER

LIST OF TABLES

LIST OF FIGURES

FIGURE Page

CHAPTER 1

INTRODUCTION

Introduction to Relativistic Quantum Mechanics

The foundation of all of modern physics rests on two pillars: the theory of relativity and the theory of quantum mechanics (QM). Born from the same generation of scientists, these two sibling theories have been at odds for over 100 years, despite their successes.

The theory of relativity lives in space-time, where time and space are treated symmetrically and the system is Lorentz invariant. Physical systems are described by 4-vectors propagating through the infinite space-time field [1].

Quantum Mechanics lives in the Hilbert space where time and space are treated asymmetrically and the system is not Lorentz invariant. Physical systems are described by two important concepts: wave functions and operators. Wave functions represent the state of the system at a given time. Operators represent physical observables of the system. Observables of physical systems are described by the eigenvalues of an operator acting upon the wave function [2].

The turn of the 20th century led to a revolution in physics. Planck is often credited as the initial founder of QM. He realized that light and other electromagnetic waves were emitted in discrete packets of energy. Einstein applied this idea to classical electromagnetic waves in blackbody radiation. By showing the change in entropy of an ideal gas consisted of independent particles, Einstein reached the conclusion that light itself is composed of irreducible finite amounts of energy and thus was able to explain the photoelectric effect [2, 3].

The same year he published his paper on the photoelectric effect, which would later earn him the Nobel prize, Einstein published his theory of special relativity. Motivated by inconsistencies of Newtonian mechanics with Maxwell's equations, and the failure of the Michelson-Morley experiment to detect the aeather, Einstein developed his theory to describe the mechanics of systems involving motions near the speed of light [3].

Twenty years later in 1925, Schrödinger published his famous wave equation. In his original publication, Schrödinger described how he solved an equation for an electron in a Coulomb field using de Broglie plane waves. However, this initial relativistic equation failed to produce eigenvalues that matched accepted energy quantum states for the hydrogen atom. Schrödinger was able to overcome this by disregarding relativity. His famous non-relativistic wave equation, which we now call the time independent Schrödinger equation, gave exact eigenvalue energies for the hydrogen-like atoms in accordance with Rydberg's law. Schrödinger eventually returned to incorporate relativity into his wave equation but not before the same equation was independently discovered by numerous others [4, 5].

The Klein-Gordon Equation

In 1921, Theodor Kaluza proposed a unified field theory of gravitation and electromagnetism built around the idea of a fifth dimension in space-time. Adding a fifth dimension to Einstein's theory allowed Kaluza to incorporate Maxwell's equations. Kaluza's 5-dimensional theory yields the same 4-dimensional Einstein field equations, as well as the Maxwell equations for the electromagnetic field and an equation for the scalar field. Kaluza's original hypothesis was purely classical and extended discoveries of general relativity. Oscar Klein applied a quantum mechanical interpretation for Kaluza's hypothesis [4].

Klein believed that the motion of electrons could be represented by self-interfering waves. Klein proposed to express quantum conditions in the five-dimensional unified theory of Kaluza. His aim was to unify electromagnetism, gravitation and QM in one equation. This was the birth of Kaluza-Klein theory, the precursor to string theory. Klein published his results in April 1926. This was the first time a relativistic quantum mechanical equation appeared in print [4].

Walter Gordon was one of the first scientists to study Klein's equation. By applying it to the Compton effect, Gordon was able describe the discrete transfer of momentum and energy of the incident radiation. Gordon calculated the current and charge densities by adopting the method used by Schrödinger. For the general case with the presence of electromagnetic fields, Gordon was able to write the charge and current densities as a four-vector [4].

Due to the efforts of both these scientists, Klein's original equation has become known as the Klein-Gordon equation. It is the standard relativistic quantum mechanical equation for spin-zero particles.

Derivation of the Klein-Gordon Equation

QM starts with a Hamiltonian

$$H = \frac{p^2}{2m} + V \tag{1.1}$$

and the time dependent non-relativistic Schrödinger equation

$$-i\hbar\frac{\partial \psi}{\partial t} + H\psi = 0 \tag{1.2}$$

where H is the Hamiltonian of the system and ψ is the wavefunction. Relativistic considerations for the energy-momentum relation give

$$p_1^2 + p_2^2 + p_3^2 + p_4^2 = -mc^2 \tag{1.3}$$

where $x = x_1$, $y = x_2$, $z = x_3$ and $ict = x_4$. If we apply the quantum operator interpretation

$$p_i = -i\hbar\frac{\partial}{\partial x_i}, \tag{1.4}$$

we can quantize the 4-momentum. Further application of a wavefunction allows us to rewrite equation (1.3) in a quantum mechanical form:

$$-\hbar^2(\frac{\partial^2 \psi}{\partial x_1^2} + \frac{\partial^2 \psi}{\partial x_2^2} + \frac{\partial^2 \psi}{\partial x_3^2} + \frac{\partial^2 \psi}{\partial x_4^2}) = -m^2c^2\psi. \tag{1.5}$$

After rearranging and rewriting in a more concise form, we arrive at the Klein-Gordon equation for a free particle

$$\left(-\frac{1}{c^2}\frac{\partial^2}{\partial t^2}+\nabla^2-\frac{m^2c^2}{\hbar^2}\right)\Psi(r,t)=0. \tag{1.6}$$

The result is an equation that is similar to the time dependent Schrödinger equation (1.2) but contains a second order time derivative. The probability density and current density are given by

$$\rho=\frac{i\hbar}{2mc^2}\left(\psi^*\frac{\partial\psi}{\partial t}-\psi\frac{\partial\psi^*}{\partial t}\right), \tag{1.7}$$

$$j=-\frac{i\hbar}{2m}\left(\psi\nabla\psi^*-\psi^*\nabla\psi\right) \tag{1.8}$$

respectively [5].

Problems with the Klein-Gordon Equation

Early researchers discovered many problems related to the Klein-Gordon equation. First, the existence of the second order time derivative in equation (1.6) violated one of the basic postulates of QM. The time evolution of a quantum mechanical system should be governed by the time dependent Schrödinger equation (1.2), which is first order in time. The existence of this second order time derivative in the Klein-Gordon equation violates this postulate. To determine the state of the equation at any given time, knowledge of both the first and second derivatives are required. In short, applying a quantum mechanical interpretation to the basic relativistic relations results in something that violates the laws of QM. Thus the Klein-Gordon equation is not a legitimate quantum mechanical equation.

The second order time derivative also causes problems with the interpretation of the probability density ρ and the probability current j. The probability density ρ contains time derivatives. Thus in general, the norm of a state

$$\langle \psi, t \,|\, \psi, t \rangle = \int d^3x \, \langle \psi, t \,|\, x \rangle \, \langle x \,|\, \psi, t \rangle = \int d^3x \psi^*(x) \psi(x) \tag{1.9}$$

is not time independent. This means that the probability density is not constrained to be positive and cannot represent a probability density distribution. In short, probability is not conserved. Thus neither ρ nor j can be interpreted as probabilistic quantities [5,6].

Finally, it can be easily seen that the Klein-Gordon equation leads to both positive and negative energy solutions. The positive solutions were taken to be particle wave functions. However, initially the negative solutions were not understood. It was only later that it was discovered these states could represent antiparticle wave functions [4,5].

The issues around the Klein-Gordon equation left many physicists wary of it's use. The Klein-Gordon equation does not explicitly involve a Hamiltonian operator. Instead it depends on the square of such an operator. Thus its relation to the Heisenburg picture and the Heisenburg equations of motion remain unclear. Many believe it does not properly correspond to quantum mechanics at all [7]. Still, with the success of its explanation of the Compton effect, its ability to explain spin zero particles, and its more intuitive explanation for anti-particles, researchers were reluctant to give the Klein-Gordon equation up and have found interpretations that are adequate [4–6].

Feshbach-Villars Solution Method to Klein-Gordon

In 1958, Herman Feshbach and Felix Villars came up with a solution that effectively linearized the time derivative of the Klein-Gordon equation while preserving the second order dependence in coordinate space. By splitting the wave function up into two components, they were able to represent the Klein-Gordon equation in terms of two coupled, Schrödinger-like equations with first order time derivatives [8]. These equations are known as the Feshbach-Villars (FV0) equations. Due to the coupling of the kinetic energy terms, even at asymptotic distances, they are difficult to solve.

In this work, the Green's operator for the FV0 equations with a Coulomb potential was calculated by using matrix continued fractions. Using this method, we are able to solve relativistic quantum mechanical problems of a spin-zero particle in a Coulomb plus short-range potential with a high level of accuracy.

First, we outline the theoretical foundation which this thesis was built on. Then we extend this foundation to developing a new method for approximating arbitrary potentials. Finally we solve the Feshbach-Villars equation for spin-zero particles with an arbitrary potential by making use of matrix continued fractions.

CHAPTER 2

FOUNDATIONAL METHODS

Green's Operator

A quantum mechanical system is completely described by the Hilbert space and the Hamiltonian H. However, in practical calculations, the infinite dimensional Hilbert space is often truncated and the calculations are performed on a finite subset of the basis. This truncation is variational and the exact results are reached as the truncated basis approaches the complete basis set.

The dynamics of a quantum mechanical system can also be fully described by the Green's operator, $G(z) = (E - H)^{-1}$, where E is the energy of the system. Many fundamental equations in physics are formulated as integral equations with Green's operators in their kernels. These integral equations offer certain advantages over the more familiar differential equations like the Hamiltonian because they automatically incorporate boundary conditions. The poles of the Green's operator are the eigenvalues of the Hamiltonian and the residue are the projection onto the subspace spanned by the eigenfuctions. If at some energy, the Green's operator is singular, then it is also singular in any physically interesting finite subspace representation. The poles of the Green's operator are insensitive to such a physically relevant truncation of the Hilbert space. Despite this, differential equations are more extensively used in practical calculations because in general, the integral equations are much more complicated to work with than the corresponding terms in the Hamiltonian [9, 10].

If a Hamiltonian is represented in a countable infinite basis by an $\infty \times \infty$ matrix, the Green's operator is the inverse of an $\infty \times \infty$ matrix. Working with $\infty \times \infty$ matrices is not very encouraging but they can be inverted in some special cases [9].

This thesis relies on the work done by Konya, Levai and Papp [10]. They showed that if a matrix $J = (z - H)$ is of a Jacobi type (i.e. infinite symmetric tridiagonal matrix), then an $N \times N$ representation of the Green's operator, G_n, can be constructed from the $N \times N$ representation of J, plus a continued fraction. The matrix $(G_n)^{-1}$ is almost identical to J_n, with the only difference being a continued fraction is added to the $N \times N$ term. They demonstrated their approach by solving the Coulomb Green's matrix in the Coulomb-Strumian (CS) basis [10].

The Coulomb-Sturmian Basis

The CS functions are the solutions of the Strum-Liuoville problem,

$$\left(-\frac{d^2}{dr^2} + b^2 + \frac{l(l+1)}{r^2} - \frac{2b(n+l+1)}{r} \right) \langle r|nl;b\rangle = 0 \tag{2.1}$$

where $b > 0$ is a parameter, $n = 0, 1, 2, ...$ is the radial quantum number and $l = 0, 1, 2, ...$ is the orbital quantum number. In coordinate space, the CS functions are given by

$$\langle r|nl;b\rangle = \left[\frac{n!}{(n+2l+1)!} \right]^{1/2} e^{-br} (2br)^{l+1} L_n^{2l+1}(2br), \tag{2.2}$$

where L_n^α is an assoicated Laguerre polynomial.

The CS functions form a basis and given

$$\langle r\,|\,\tilde{n}\rangle = \frac{1}{r}\langle r\,|\,n\rangle \tag{2.3}$$

we obtain orthogonality and completeness relations

$$\left\langle \tilde{n}\,|\,n'\right\rangle = \left\langle n\,|\,\tilde{n}'\right\rangle = \left\langle n\left|\frac{1}{r}\right|n'\right\rangle = \delta_{nn'} \tag{2.4}$$

$$\sum_{n=0} |n\rangle\langle\tilde{n}| = \sum_{n=0} |\tilde{n}\rangle\langle n| = \mathbf{1}. \tag{2.5}$$

The straightforward calculation of the overlap of the CS states gives

$$\left\langle n\middle|n^{'}\right\rangle = \left\langle n^{'}\middle|n\right\rangle = \begin{cases} \frac{1}{b}(n+l+1) & for\ n^{'}=n, \\ -\frac{1}{2b}\sqrt{n^{'}(n^{'}+2l+1)} & for\ n^{'}=n+1, \\ 0 & for\ n^{'}>n+1. \end{cases} \tag{2.6}$$

Applying this relation to equation (2.1), we can derive the CS matrix elements of a

Hamiltonian H:

$$\left\langle n \middle| H \middle| n^{'} \right\rangle = \left\langle n^{'} \middle| H \middle| n \right\rangle = \begin{cases} \frac{b}{2}(n+l+1) & for\ n^{'} = n, \\ -\frac{b}{4}\sqrt{n^{'}(n^{'}+2l+1)} & for\ n^{'} = n+1, \\ 0 & for\ n^{'} > n+1. \end{cases} \tag{2.7}$$

These relations both show a Jacob-matrix structure. Thus from equations (2.4),(2.6) and (2.7), it follows that the Hamiltonian, is represented by a tridiagonal matrix on the CS basis [11, 12].

Konya, Levai and Papp demonstrated that Hamiltonians represented in a discrete basis with Jacobi-matrix structure, have a corresponding Green's matrix that can be calculated on the whole complex energy plane by a continued fraction. The coefficients of the continued fraction are related to the elements of the Jacobi matrix [11–13].

Continued Fraction Representation

Formally the Green's operator is defined by

$$G(z)(z-H) = (z-H)G(z) = 1 \tag{2.8}$$

where z is a complex number and H is the Hamiltonian.

We assume the operator $J = z - H$ has an infinite symmetric tridiagonal (i.e. Jacobi) structure in some discrete basis. Thus equation (2.8) becomes:

$$\begin{pmatrix} J_{0,0} & J_{0,1} & 0 & 0 & \dots \\ J_{1,0} & J_{1,1} & J_{1,2} & 0 & \dots \\ 0 & J_{2,1} & J_{2,2} & J_{2,3} & \dots \\ 0 & 0 & J_{3,2} & J_{3,3} & \dots \\ \vdots & \vdots & \vdots & \vdots & \ddots \end{pmatrix} \times \begin{pmatrix} G_{0,0} & G_{0,1} & G_{0,2} & G_{0,3} & \dots \\ G_{1,0} & G_{1,1} & G_{1,2} & G_{1,3} & \dots \\ G_{2,0} & G_{2,1} & G_{2,2} & G_{2,3} & \dots \\ G_{3,0} & G_{3,1} & G_{3,2} & G_{3,3} & \dots \\ \vdots & \vdots & \vdots & \vdots & \ddots \end{pmatrix} = \begin{pmatrix} 1 & 0 & 0 & 0 & \dots \\ 0 & 1 & 0 & 0 & \dots \\ 0 & 0 & 1 & 0 & \dots \\ 0 & 0 & 0 & 1 & \dots \\ \vdots & \vdots & \vdots & \vdots & \ddots \end{pmatrix} \tag{2.9}$$

Due to the tridiagonal form, we can reduce the sum to just three terms

$$J_{n,n-1}G_{n-1,m} + J_{n,n}G_{n,m} + J_{n,n+1}G_{n+1,m} = \delta_{n,m}. \tag{2.10}$$

where $n = 0,1,...,N$ and $m = 0,1,...,N$.

If $n < N$ then only terms from $G^{(N)}$ contribute to the sum. At the limit of $n = N$, where N is the desired dimension of the truncated subspace, an extra matrix element $G_{N+1,m}$ outside the truncated subspace is need:

$$J_{N,N-1}G_{N-1,m} + J_{N,N}G_{N,m} + J_{N,N+1}G_{N+1,m} = \delta_{N,m}. \tag{2.11}$$

We can formally eliminate the elements outside of $G^{(N)}$ by expressing equation (2.11)

$$J_{N,N-1}G_{N-1,m} + \left[J_{N,N} + J_{N,N+1}\frac{G_{N+1,m}}{G_{N,m}} \right] G_{N,m} = \delta_{N,m}. \tag{2.12}$$

To calculate the ratio of $\frac{G_{N+1,m}}{G_{N,m}}$ we use equation (2.10) to get the following relation:

$$J_{N+1,N}G_{N,m}+J_{N+1,N+1}G_{N+1,m}+J_{N+1,N+2}G_{N+2,m}=0. \tag{2.13}$$

After rearranging we get the following relation

$$\left(-\frac{1}{J_{N+1,N}}\frac{G_{N+1,m}}{G_{N,m}}\right)^{-1}=J_{N+1,N+1}-J_{N+1,N+2}\left(-\frac{1}{J_{N+2,N+1}}\frac{G_{N+2,m}}{G_{N+1,m}}\right)J_{N+2,N+1}. \tag{2.14}$$

After repeated application of this, it can be seen that the modified Jacobi matrix is the inverse of $G^{(N)}$:

$$(G^{N})^{-1}=J^{(N)}-\delta_{i,N}\delta_{j,N}J_{N,N+1}^{2}C_{N+1} \tag{2.15}$$

where C_{N+1} is a continued fraction defined as

$$C_{N+1}=-\frac{1}{J_{N+1,N}}\frac{G_{N+1,m}}{G_{N,m}}. \tag{2.16}$$

Using this notation, we can now rearrange equation 2.13 as

$$C_{N+1}=(J_{N+1,N+1}-J_{N+1,N+2}C_{N+2}J_{N+2,N+1})^{-1}. \tag{2.17}$$

Notice this continued fraction does not depend on the index m and the correction term to the $J_{N,N}$ term is the same for all m. One can effectively eliminate the m dependence by use of the continued fraction.

Consider two sequences, $\{\, a_n(z) \,\}_1^\infty$ and $\{\, b_n(z) \,\}_0^\infty$, of complex valued functions defined on the complex plane. Given the linear fractional transformation $s_n(w_n, z)$ as

$$s_n(w_n, z) = \frac{a_n(z)}{b_n(z) + w_n} \tag{2.18}$$

with $n \geq 1$, $s_0(w_0, z) = b_0(z) + w_0$ and

$$S_n(w_n, z) = S_{n-1}(s_n(w_n, z), z) \tag{2.19}$$

where $S_0(w_0, z) = s_0(w_0, z)$. Then a continued fraction is an ordered pair

$$((\{\, a_n \,\}, \{\, b_n \,\}), \{\, f_n(z) \,\}) \tag{2.20}$$

where $\{\, f_n(z) \,\}$ is given by

$$f_n(z) = S_n(0, z). \tag{2.21}$$

It is a recursive relation in which terms in the sequence are defined by the terms after it:

$$S_{n+1}(w_n,z) = \cfrac{a_0(z)}{b_0(z) + \cfrac{a_1(z)}{b_1(z) + \cfrac{a_2(z)}{b_2(z) + \ddots \cfrac{a_n(z)}{b_n(z) + \cfrac{a_{n+1}(z)}{b_{n+1}(z) + w_n(z)}}}}}. \tag{2.22}$$

$S_n(w_n,z)$ is called the *n*th approximant of the continued fraction with respect to the $\{\, w_n \,\}_0^\infty$ complex series [12]. It is safe to assume the sequence described by equation (2.22) converges between 0 and ∞. If the value of w_n is ∞, our approximation is good to the b_n term. If the value of w_n is zero, our approximation is good to the $\frac{a_{n+1}}{b_{n+1}}$ term. Either case results in a similar approximation and thus demonstrates the effectiveness of a continued fraction approximation.

The continued fraction representation of the Green's inverse operator given by (2.15) is convergent for bound-state energies. At eigenvalue energies the determinant of the $G_n(E)$ is singular and the determinant of $(G_N(E))^{-1}$ does not exist. Thus we can consider $(G_N(E))^{-1}$ as an improved Hamiltonian, which irrespective of N, provides the correct eigenvalues. In this way we accomplish a kind of "packing" of the $\infty \times \infty$ matrix into an $N \times N$ matrix, where N is not necessarily big.

Matrix Continued Fraction Representation

This approach was extended to infinite symmetric band matrices. An infinite

$$\begin{bmatrix} \begin{pmatrix} X & X \\ X & X \end{pmatrix} & \begin{pmatrix} X & X \\ X & X \end{pmatrix} & \begin{pmatrix} 0 & 0 \\ 0 & 0 \end{pmatrix} & \begin{pmatrix} 0 & 0 \\ 0 & 0 \end{pmatrix} \\ \begin{pmatrix} X & X \\ X & X \end{pmatrix} & \begin{pmatrix} X & X \\ X & X \end{pmatrix} & \begin{pmatrix} X & X \\ X & X \end{pmatrix} & \begin{pmatrix} 0 & 0 \\ 0 & 0 \end{pmatrix} \\ \begin{pmatrix} 0 & 0 \\ 0 & 0 \end{pmatrix} & \begin{pmatrix} X & X \\ X & X \end{pmatrix} & \begin{pmatrix} X & X \\ X & X \end{pmatrix} & \begin{pmatrix} X & X \\ X & X \end{pmatrix} \\ \begin{pmatrix} 0 & 0 \\ 0 & 0 \end{pmatrix} & \begin{pmatrix} 0 & 0 \\ 0 & 0 \end{pmatrix} & \begin{pmatrix} X & X \\ X & X \end{pmatrix} & \begin{pmatrix} X & X \\ X & X \end{pmatrix} \end{bmatrix}$$

FIGURE 1. An example of the structure of a block tridiagonal matrix, where X represents a non-zero element.

symmetric band-matrix can be considered as a Jacobi matrix of block matrices.

Therefore, we can represent the Green's operator in a similar manner as before:

$$(G^N)^{-1}_{i,j} = J^N_{i,j} - \delta_{i,N}\delta_{j,N}J_{N,N+1}C_{N+1}J_{N+1,N} \tag{2.23}$$

but now $J_{i,j}$ are block matrices and C_{N+1} is now a matrix continued fraction defined by

$$C_{N+1} = (J_{N+1,N+1} - J_{N+1,N+2}C_{N+2}J_{N+2,N+1})^{-1}. \tag{2.24}$$

A matrix continued fraction is similar to a continued fraction with the numbers of the continued fraction replaced by $m \times m$ matrices (see fig. 1). Matrix division is undefined and commutativity is not given so the procedure is a bit more tedious than when working with continued fractions but the theory is the same. An accurate representation of the whole Hilbert space can be expressed in this way. Using this method, the Green's operator for Hamiltonian containing kinetic energy, Coulomb and polynomial potentials have been evaluated [12].

CHAPTER 3

APPROXIMATION OF THE POTENTIAL

A Hamiltonian, besides the Coulomb and some polynomials potential, may contain a short-range potential as well. A general short-range potential in a discrete basis representation is certainly not tridiagonal; it may not even be block-tridiagonal. But for any reasonable potential, the matrix representation looks like a ridge: the matrix elements are much bigger if the n and n' are close and become negligible otherwise, similar to a band-matrix. Therefore, the technique developed before may be applicable for finding a faithful matrix representation of a general short-range potential.

This section outlines the brief report published in research by Brown, Grefe and Papp [9]. The aim is to find a low-N representation of the short-range potential such that it carries the information of the whole Hilbert-space representation. This goal is accomplished through the inverse of the potential operator.

We present our results in the Coulomb-Sturmian basis representation, but we believe that the results are valid for any discrete basis provided the matrix exhibits a ridge-like structure. The method of approximating the potential on the Coulomb-Sturmian basis has quite a long history. It has successfully been applied to various problems, including the solution of the Faddeev equations with a Coulomb potential [14, 15] and confining potential [16]. This chapter introduces the physical system and outline previous schemes for approximating the potential. Finally we apply the inverse matrix idea to matrix with ridge-like structure and summarize the results.

Solution of the Lippmann-Schwinger Equation

We consider a Hamiltonian with a Coulomb, v^C, plus short-range, $v^{(s)}$, potential. The bound states are the solutions of the homogeneous Lippmann-Schwinger equations

$$|\psi\rangle = g_l^C(E) v_l^{(s)} |\psi\rangle, \tag{3.1}$$

while the scattering states are the solutions of the inhomogeneous Lippmann-Schwinger equations

$$|\psi^{(\pm)}\rangle = |\phi_l^{C(\pm)}\rangle + g_l^C(E \pm i\varepsilon) v_l^{(s)} |\psi^{(\pm)}\rangle \tag{3.2}$$

where E is the energy, l is the angular momentum, $g_l^C(E) = (E - h_l^0 - v^C)^{-1}$ is the Coulomb Green's operator, h_l^0 is the kinetic energy and ϕ_l^C is the Coulomb scattering state.

The finite dimensional representation of the short-range potential is given by

$$v_l^{(s)} = \sum_{nn'}^{N} |\widetilde{nl}\rangle \underline{v}_{l,nn'}^{(s)N,N} \langle\widetilde{n'l}| \ , \tag{3.3}$$

where $v_{l,nn'}^{(s)} = \langle nl|v_l^{(s)}|n'l\rangle$. Now the Lippmann-Schwinger equations (3.1) and (3.2) become matrix equations

$$\underline{\psi} = \underline{g}_l^C \underline{v}_l^{(s)} \underline{\psi} \tag{3.4}$$

and

$$\underline{\psi} = \underline{\phi}_l^C + \underline{g}_l^C \underline{v}_l^{(s)} \underline{\psi}, \tag{3.5}$$

respectively, where the matrices and vectors are underlined. Some rearrangement gives

$$((\underline{g}_l^C)^{-1} - \underline{v}_l^{(s)})\underline{\psi} = 0 \tag{3.6}$$

and

$$((\underline{g}_l^C)^{-1} - \underline{v}_l^{(s)})\underline{\psi} = (\underline{g}_l^C)^{-1}\underline{\phi}_l^C \ , \tag{3.7}$$

i.e. the homogeneous Lippmann-Schwinger equation becomes a homogeneous algebraic equation and the inhomogeneous Lippmann-Schwinger equation becomes an inhomogeneous algebraic equation. The homogeneous algebraic equation is solvable if the determinant is zero

$$|(\underline{g}_l^C)^{-1}(E) - \underline{v}_l^{(s)}| = 0. \tag{3.8}$$

This condition provides the eigenvalues and the solution of (3.6) provides the eigenvectors. The solution of the inhomogeneous algebraic equation gives the scattering state $\underline{\psi}$.

The matrix $(\underline{g}_l^C)^{-1}$ can be calculated by using (2.10)

$$(\underline{g}_l^C)^{-1} = \underline{J}^C - \delta_{i,N}\delta_{j,N}J_{N,N+1}^2 C_{N+1} \ . \tag{3.9}$$

Here $J(E) = (E - h_l^0 - v^C)$ and $v^C = Z/r$. The matrix $\underline{J}^C$ is symmetric tridiagonal, and the nonzero elements are given by

$$\underline{J}^C_{i,i} = 2(i+l+1)\frac{\hbar^2(k^2-b^2)}{4\mu b} - Z \tag{3.10}$$

and

$$\underline{J}^C_{i,i+1} = -\sqrt{(i+1)(i+2l+2)}\frac{\hbar^2(k^2+b^2)}{4\mu b}\ , \tag{3.11}$$

where μ is the reduced mass and $k = \sqrt{2\mu/\hbar^2 E}$. In this particular case the continued fraction can be summed up to a ratio of hypergeometric functions

$$\begin{aligned} C_{N+1} \quad &= -\frac{4m/\hbar^2 b}{(b-ik)^2(N+l+2+i\gamma)} \\ &\times \frac{{}_2F_1\left(-l+i\gamma, N+2; N+l+3+i\gamma; \left(\frac{b+ik}{b-ik}\right)^2\right)}{{}_2F_1\left(-l+i\gamma, N+1; N+l+2+i\gamma; \left(\frac{b+ik}{b-ik}\right)^2\right)}\ , \end{aligned} \tag{3.12}$$

where $\gamma = Z\mu/(\hbar^2 k)$ [13]. The analytic evaluation of $\underline{\phi}^C_l$ has been presented before in [10].

This representation of $(\underline{g}^C_l)^{-1}$ is exact and analytic. Even a very low-rank matrix gives an account for the complete spectrum of the Coulomb Hamiltonian. Fig. 2 shows the determinant of the 3×3 $(\underline{g}^C_l)^{-1}$ matrix for Coulomb Hamiltonian with $l = 0$, $Z = -1$, $\mu = 1$ and $\hbar = 1$. The exact eigenvalues are $E_n = -1/(2n^2)$. The figure shows the energy range corresponding to the (E_{90}, E_{100}) interval. We can see that the numerical zeros are at the exact locations even in this extreme case.

In this approach the only approximation is the finite-basis representation of the

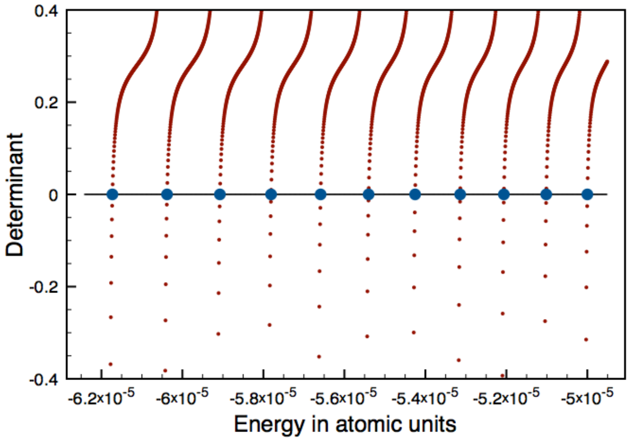

FIGURE 2. The zeros of for a hydrogen system in atomic units. The zeros of $|\underline{g}_0^C(E)|^{-1}$ of a 3×3 basis for the Coulomb Hamiltonian in atomic units in the energy range (E_{90}, E_{100}). The large dots represent the exact eigenvalues.

potential, since the evaluation of $\underline{g}_l^C$ and $\underline{\phi}_l^C$ is exact and analytic. Therefore both the bound and scattering state wave function ψ and $\psi^{\pm}$ possess the exact Coulomb-like asymptotic behavior [17].

Finite-rank potentials have a long history in physics (see eg. Ref. [18]). Various schemes have been proposed. Most of them use some form factors which allow for an easy and exact evaluation of the matrix elements of the Green's operator. The use of Coulomb-Sturmian functions offers several advantages. Since they form a basis, the convergence of the approximation is guaranteed. More importantly, it works with Coulomb-like potentials, unlike the majority of approaches.

The Example Problem: Nucleon-Nucleon Potential

To illustrate the method we consider a typical nucleon-nucleon potential, the Malflet-Tjon potential. This potential has a strong repulsive core and an attractive tail, like most of the potentials in physics. The Malflet-Tjon potential is given by

$$v^{(s)} = v_1 \exp(-\beta_1 r)/r + v_2 \exp(-\beta_2 r)/r \tag{3.13}$$

with $v_1 = 1438.720\,\mathrm{MeV}$, $\beta_1 = 3.11\,\mathrm{fm}^{-1}$, $v_2 = -626.885\,\mathrm{MeV}$, $\beta_2 = 1.55\,\mathrm{fm}^{-1}$. The other parameters in the model are charge parameter $Z = e^2 = 1.44\,\mathrm{MeV\ fm}$, $\hbar^2/m = 41.47\,\mathrm{MeV}$ / amu and nucleon reduced mass $\mu = 1/2\,\mathrm{amu}$. The Malflet-Tjon potential with these conditions give the experimental binding energy for deuteron. We used $b = 3\,\mathrm{fm}^{-1}$, which is around the optimum. We note that the rate of convergence is rather insensitive to the choice of b within a rather broad interval.

Figure 3 shows the Malflet-Tjon potential in a 20 × 20 basis. We can see that the matrix representation exhibits a ridge-like structure and the dominant matrix elements decrease only very slowly. So, if we truncate the basis to this size, we chop down the tail of the matrix and we neglect terms which are not small at all. Consequently, this representation results in a slow convergence.

We have to note here that there had been approaches before to improve the situation. Inspired by Lanczos filtering, it has been proposed to multiply the potential matrix by some function which suppress the higher elements [19, 20]

$$\underline{\tilde{v}}^{N}_{i,j} = \sigma_i^{N+1} \underline{v}^{N,N} \sigma_j^{N+1}, \tag{3.14}$$

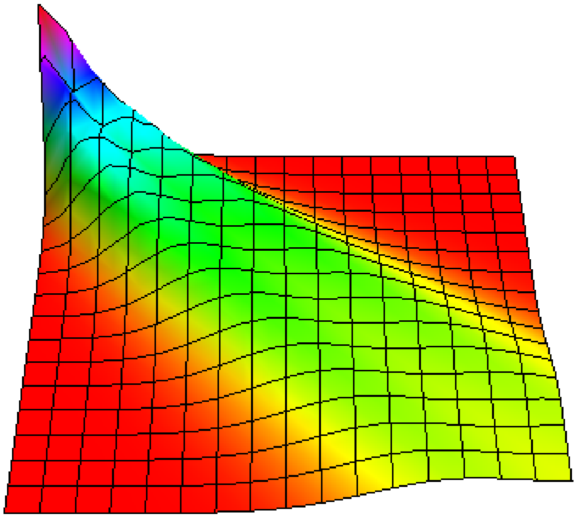

FIGURE 3. Coulomb-Sturmian matrix elements of the Malflet-Tjon potential. Basis size 20×20. The upper left corner represents the $v_{0,0}$ element, while the lower right hand corner represents the $v_{20,20}$ element.

where

$$\sigma_i^N = \frac{1-\exp(-[\alpha(i-N-1)/(N+1)]^2)}{1-\exp(-\alpha^2)} \tag{3.15}$$

with $\alpha \sim 6$. This approach results in a transformed matrix shown in Fig. 4.

In the other approach two Hilbert-space bases has been adopted [21, 22]

$$\underline{\hat{v}}^N = \underline{O}\,\underline{v}^{N,N}\,\underline{O}', \tag{3.16}$$

where $\underline{v}^{N,N}$ has been calculated with basis parameter b_1 and $\underline{O} = (\langle \widetilde{nl;b_1}|n'l;b_2\rangle)^{-1}$. The potential matrix $\underline{\hat{v}}$ with $b_1 = 2.5\,\mathrm{fm}^{-1}$ and $b_2 = 3.5\,\mathrm{fm}^{-1}$ is shown in Fig. 5. It is interesting to note that this approach also utilizes the inverse of the potential operator [21]. Our approach is however different, as we are going to see below.

We can see that both methods basically suppress the higher index elements of the

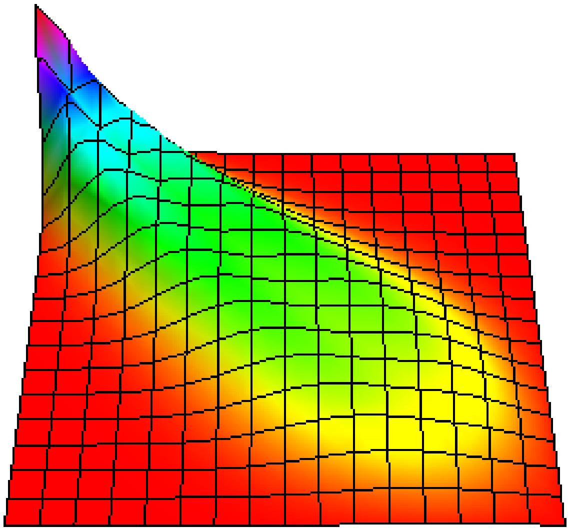

FIGURE 4. Malflet-Tjon potential matrix elements modified with a form factor. Potential matrix $\underline{\tilde{v}}^{20}$. The matrix of Fig. 3 has been modified by the σ factors of Eq. (3.15). Again, the upper left corner represents the $v_{0,0}$ element, while the lower right hand corner represents the $v_{20,20}$ element.

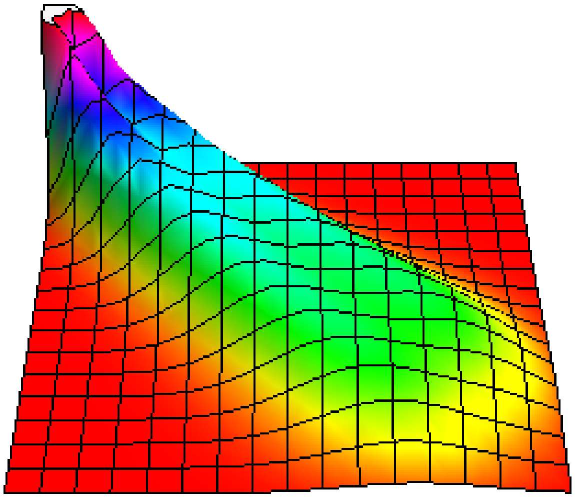

FIGURE 5. Malflet-Tjon potential matrix elements double basis representation. Potential matrix $\underline{\hat{v}}^{20}$ from double-basis representation of Eq. (3.16). The upper left corner represents the $v_{0,0}$ element, while the lower right hand corner represents the $v_{20,20}$ element.

matrix. Now the transition to the neglected terms is smooth. We found that among these two methods, the one with two bases gives a faster convergence [22].

Approximation through the Inverse

Previous research has shown that a good approximation of the Hamiltonian can be achieved by considering it on an infinite basis representation and then by rolling up the tail of the band matrix into a matrix continued fraction [10]. Here we try a similar procedure with the potential operator. First we calculate the Coulomb-Sturmian matrix elements of $v^{(s)}$ on a basis of N' size, invert the matrix, then truncate it to $N \leq N'$, and finally invert the matrix again. We denote the resulting matrix by $\underline{v}^{N,N'}$ where

$$\underline{v}^{N,N'} = (((\underline{v}^{(s)N',N'})^{-1})^{N,N})^{-1}. \tag{3.17}$$

Figures 6, 7 and 8 display $\underline{v}^{20,21}$, $\underline{v}^{20,22}$ and $\underline{v}^{20,27}$, respectively. We can see that as N' increases, the matrix elements around the corner become more and more suppressed. Thus if we truncate the matrix to $N \times N$ size, we neglect terms which are small. We can also see from these pictures that this procedure in accordance with Eq. (2.23) modifies mostly the lower right corner of the potential matrix. It is also interesting to see that in Fig. 6, even stepping out just by one basis state, and truncating back, results in a dramatic reduction of the matrix elements around the lower right corner.

Figure 9 shows the convergence of the deuteron binding energy with $\underline{v}^{20,N'}$ and $\underline{v}^{N',N'}$ as a function of N'. We can see that our approach of inverting and cutting back the potential matrix is more advantageous than keeping the original bigger matrix. Our

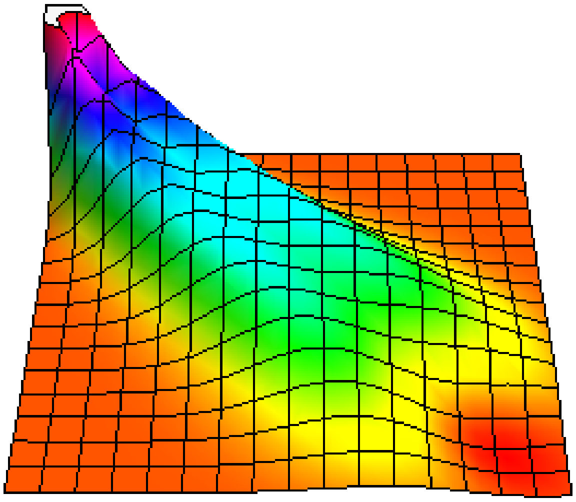

FIGURE 6. Coulomb-Sturmian matrix elements of the Malflet-Tjon potential with one basis step out. $\underline{v}^{20,21}$ (i.e. one basis step out). The upper left corner represents the $v_{0,0}$ element, while the lower right hand corner represents the $v_{20,20}$ element.

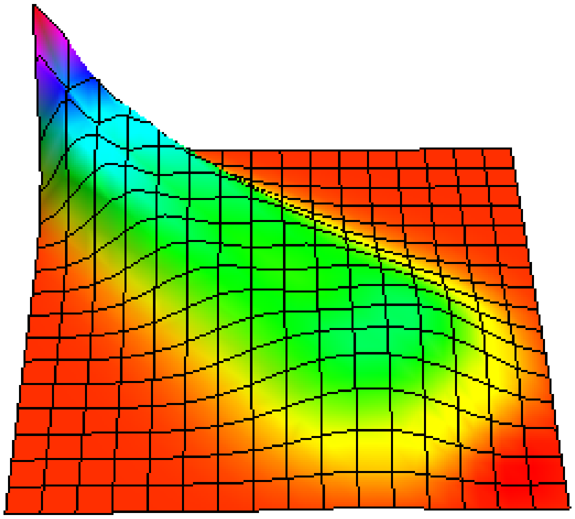

FIGURE 7. Coulomb-Sturmian matrix elements of the Malflet-Tjon potential with two basis step out. $\underline{v}^{20,22}$ (i.e. two basis step out). The upper left corner represents the $v_{0,0}$ element, while the lower right hand corner represents the $v_{20,20}$ element.

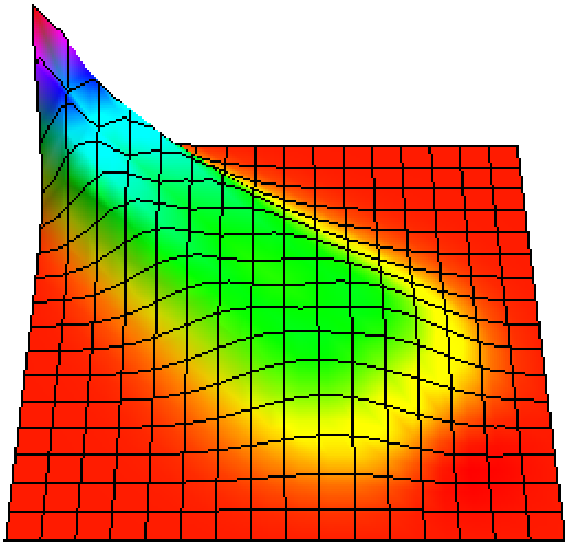

FIGURE 8. Coulomb-Sturmian Matrix Elements of the Malflet-Tjon Potential with Seven Basis Step Out. $\underline{v}^{20,27}$ (i.e. seven basis step out). The upper left corner represents the $v_{0,0}$ element, while the lower right hand corner represents the $v_{20,20}$ element.

approach gives a better approximation of the whole Hilbert space with fast and accurate convergence. We can also see that beyond $N' = N+4 \to N' = N+7$ there is no further improvement. We found the same effect with other N values and for scattering states as well. So, we fix $N' = N+7$.

Table 1 shows the convergence of the deuteron and $p-p$ scattering phase shifts at low, intermediate and high energies with increasing N. We can observe excellent results even with very low N. We observe four digit accuracy with basis representation as low as $N = 4$ and eight or nine digit accuracy with $N = 20$. The rate of convergence is better than with the double basis method and higher accuracy can be achieved.

Summary and Conclusions

In this chapter we propose a new finite-basis representation for the potential operator. The approach is inspired by recent finding concerning Green's operators. If the

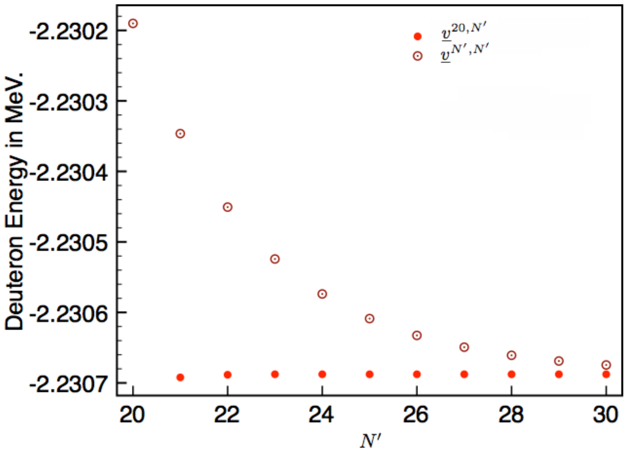

FIGURE 9. Convergence of the deuteron bound state energy with potential matrices $\underline{v}^{20,N'}$ and $\underline{v}^{N',N'}$.

asymptotic Hamiltonian is represented in a discrete basis, then for the resolvent the $\infty \times \infty$ symmetric band-matrix is inverted by a matrix continued fraction. A general potential operator is not exactly an infinite band-matrix, but it is similar. The potential matrix exhibits a ridge-like structure which looks like a band-matrix.

Based on this analogy, we proposed a numerical procedure for a finite-basis representation of the potential such that it retains some information about the whole Hilbert space. We need to calculate the matrix elements of the potential in a slightly larger basis, about $5-7$ terms larger, invert the matrix numerically, then truncate the matrix to the desired size, and finally invert again. This procedure is very straightforward, automatic, results in a fast convergence in N and provides very accurate results. Furthermore, this technique can be easily incorporated into other numerics as we will see in the next chapter. The easy of this incorporation means this technique can be applied to a wide range of problems.

TABLE 1. The Convergence of the Deuteron Bound State Energy and $p-p$ Scattering Phase Shifts at Low, Intermediate and High Energies.

N	E_d	E = 0.1 MeV	E = 1.0 MeV	E = 100 MeV
3	-2.14459561	-0.121277396	-0.708187417	0.378017184
4	-2.23413092	-0.119071149	-0.701325274	0.400336999
5	-2.22996195	-0.119221696	-0.701844279	0.406882711
6	-2.22826603	-0.119221074	-0.701711392	0.406989848
7	-2.22954511	-0.119209853	-0.701708254	0.406858120
8	-2.23027115	-0.119172562	-0.701542559	0.407291677
9	-2.23060304	-0.119165639	-0.701519683	0.407488351
10	-2.23068178	-0.119161793	-0.701503458	0.407494569
11	-2.23069092	-0.119161850	-0.701503994	0.407494183
12	-2.23068711	-0.119161857	-0.701503930	0.407498147
13	-2.23068566	-0.119161942	-0.701504323	0.407498408
14	-2.23068594	-0.119161930	-0.701504270	0.407499317
15	-2.23068671	-0.119161903	-0.701504180	0.407499210
16	-2.23068728	-0.119161894	-0.701504142	0.407499294
17	-2.23068757	-0.119161880	-0.701504093	0.407499379
18	-2.23068769	-0.119161881	-0.701504095	0.407499377
19	-2.23068773	-0.119161878	-0.701504085	0.407499387

The $N\times N$ representation of the potential was calculated from an $N+7\times N+7$ representation.

CHAPTER 4

SOLVING THE FESHBACH-VILLARS EQUATION

Feshbach-Villars Formalism

The Feshbach-Villars form of the Klein-Gordon equation originates from a 1958 publication by Herman Feshbach and Felix Villars [8]. In this paper, Feshbach and Villars develop a representation of the Klein-Gordon equation that effectively linearizes the second order time dependence and succeeded in finding a Hamiltonian formulation. The presence of the second time derivative indicates that the wave function has two degrees of freedom. By expressing these two degrees of freedom separately in the form of two coupled linear equations, a Hamiltonian can be found for the system [8].

Recall the Klein-Gordon equation (1.6). For a particle in a potential V,

$$\left(-i\hbar\frac{\partial}{\partial t}-V\right)^2\Psi(r,t)=\left(c^2\nabla^2-\frac{m^2c^4}{\hbar^2}\right)\Psi(r,t) \tag{4.1}$$

which has a second-order time dependence. In the Feshbach-Villars approach, the wave function is split into two components $\Psi=\phi+\chi$ with the components defined by

$$\phi=\frac{1}{2}\left[\left(1-\frac{V}{mc^2}\right)\Psi+i\frac{\hbar}{mc^2}\frac{\partial\Psi}{\partial t}\right] \tag{4.2}$$

$$\chi = \frac{1}{2}\left[\left(1+\frac{V}{mc^2}\right)\Psi - i\frac{\hbar}{mc^2}\frac{\partial\Psi}{\partial t}\right]. \tag{4.3}$$

From these components and the first order time dependence, one can produce Schrödinger-like equations. These equations are known as the Feshbach-Villars (FV0) equations for a spinless particle:

$$i\hbar\frac{\partial\phi}{\partial t} = \frac{p^2}{2m}(\phi+\chi) + (mc^2+V)\phi \tag{4.4}$$

$$i\hbar\frac{\partial\chi}{\partial t} = -\frac{p^2}{2m}(\phi+\chi) - (mc^2-V)\chi. \tag{4.5}$$

However, there is a cost to this approach. Since we now no longer have a single component wave function, but a two component one, we also have a matrix Hamiltonian:

$$H_{FV0} = (\tau_3 + i\tau_2)\frac{p^2}{2m} + \tau_3 mc^2 + V \tag{4.6}$$

where τ_i denote the Pauli matrices:

$$\tau_1 = \begin{pmatrix} 0 & 1 \\ 1 & 0 \end{pmatrix}, \tau_2 = \begin{pmatrix} 0 & -i \\ i & 0 \end{pmatrix}, \tau_3 = \begin{pmatrix} 1 & 0 \\ 0 & -1 \end{pmatrix}. \tag{4.7}$$

Using this representation and by defining

$$\Psi = \begin{pmatrix} \phi \\ \chi \end{pmatrix} \tag{4.8}$$

the Klein-Gordon equation can now be cast into a true Hamiltonian form:

$$i\hbar\frac{\partial\Psi}{\partial t} = H_{FV0}\Psi. \tag{4.9}$$

This Hamiltonian is not symmetric and therefore not hermitian, which is another requirement for QM. However, it does produce real eigenvalues and thus can represent a real physical observable [5,8].

From the time-dependent formalism, this equation can be expressed time-independently by quantizing energy using the QM relation

$$i\hbar\frac{\partial}{\partial t} = E. \tag{4.10}$$

Substituting this into equation (4.9) reduces the equation to a basic eigenvalue problem

$$H_{FV0}\Psi = E\Psi. \tag{4.11}$$

$$H_{FV0}\begin{pmatrix} |\phi\rangle \\ |\chi\rangle \end{pmatrix} = E\begin{pmatrix} |\phi\rangle \\ |\chi\rangle \end{pmatrix}. \tag{4.12}$$

$$G_{FV0}(E) = (E - H_{FV0})^{-1} \tag{4.13}$$

We can see that the eigenvalues of the Hamiltonian occur at the poles of the Green's operator.

However, this approach is difficult analytically. The Hamiltonian and the Green's operator live in Hilbert space, so mathematically, they are represented by infinite matrices. The goal of our work was to accurately represent these infinite matrices in a manner that allows a numerical (i.e. finite) calculation. This is done by representing the Green's operator in terms of a matrix continued fraction.

The Example Problem: Hydrogen Atom

We demonstrate our method by solving for the hydrogen atom in an arbitrary short range potential potential. The FV0 equations for Coulomb Hamiltonian are given by

$$H^{C}_{FV_0} = \begin{pmatrix} 1 & 1 \\ -1 & -1 \end{pmatrix} H_0 + \begin{pmatrix} 1 & 0 \\ 0 & -1 \end{pmatrix} mc^2 + \begin{pmatrix} 1 & 0 \\ 0 & 1 \end{pmatrix} V^C \tag{4.14}$$

where $H_0 = \frac{p^2}{2m}$ and V^C is the Coulomb potential.

Figures 10 and 11 show the matrix representation of the Green's inverse operator $J = (E - H^{C}_{FV_0})$ in the Coulomb-Strumian basis. We can see from figure 10 the matrix J has a tridiagonal structure. The higher basis states are not negligible and should be accounted for an accurate picture of the system.

There are many approximation methods used in quantum mechanics. Among the most popular are the Wentzel-Kramers-Brillouin (WKB), perturbative and variational approaches. WKB approximation is useful for approximate treatments of systems with slowly varying potentials. It is most commonly used to approximate large N eigenenergies in bound state problems. Pertubative methods rely on the existences of a small dimensionless parameters, which when taken to zero, renders the problem exactly

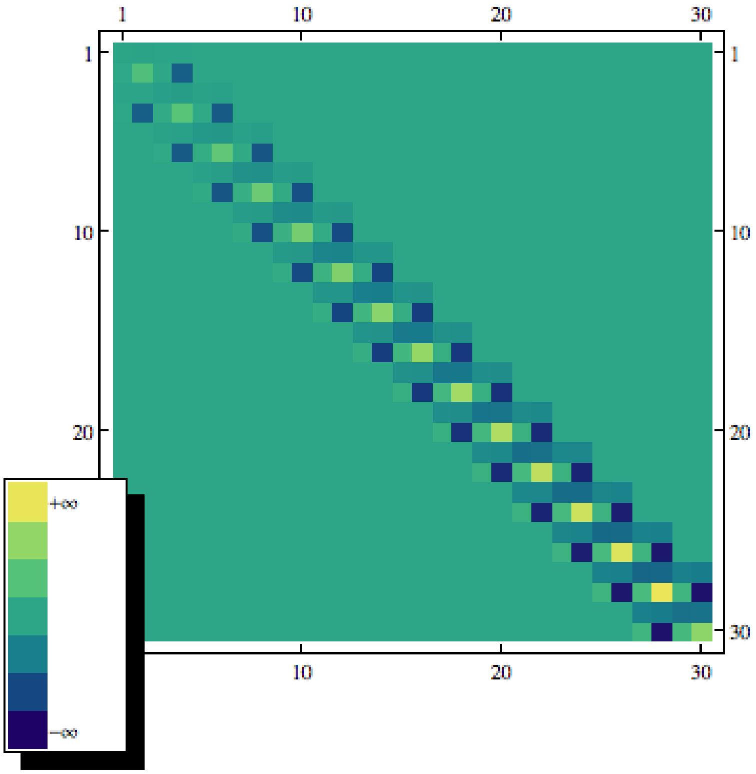

FIGURE 10. Matrix plot of the Green's inverse matrix. Matrix plot of the elements of a 30×30 Green's inverse matrix J. The upper left corner represents the $v_{0,0}$ element, while the lower right hand corner represents the $v_{30,30}$ element.

solvable. It can be used to describe non asymptotic behaviors. The variational method is useful for determining upper bound values for the eigenenergies of a system. It is useful for studying the ground state but is cumbersome at higher energy levels. Each one of these methods has its uses but limitations [2].

As discussed in chapter 2, it has been shown that if the Hamiltonian is represented by an infinite tridiagonal matrix, then the corresponding Green's operator is represented by a continued fraction [13]. It is know that the Schrödinger Hamiltonian of the Coulomb potential is tridiagonal in the Coulomb-Strumian (CS) basis. Our Hamiltonian as given in equation (4.14), is very much like the Schrödinger Hamiltonian, and has a similar

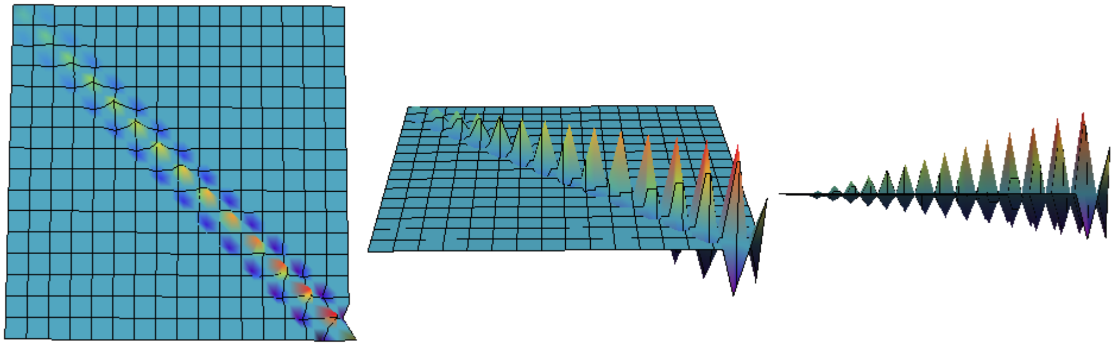

FIGURE 11. Rotational view of tridiagonal structure of the Green's inverse matrix. A 30×30 tridiagonal structure of the Green's inverse matrix J. The upper left corner represents the $v_{0,0}$ element, while the lower right hand corner represents the $v_{30,30}$ element.

behavior in the same basis. But instead of being element tridiagonal, it is block tridiagonal. This allows us to apply a similar theory as performed in prior research [13], but instead of representing the operator in terms of a continued fraction, it is represented in terms of a matrix continued fraction.

Matrix Continued Fraction Approach

Consider the formal definition of the Green's operator G for our FV0 case:

$$\begin{pmatrix} J_{0,0} & J_{0,1} & 0 & \dots \\ J_{1,0} & J_{1,1} & J_{1,2} & \dots \\ 0 & J_{2,1} & J_{2,2} & \dots \\ \vdots & \vdots & \vdots & \ddots \end{pmatrix} \times \begin{pmatrix} G_{0,0} & G_{0,1} & G_{0,2} & \dots \\ G_{1,0} & G_{1,1} & G_{1,2} & \dots \\ G_{2,0} & G_{2,1} & G_{2,2} & \dots \\ \vdots & \vdots & \vdots & \ddots \end{pmatrix} = \begin{pmatrix} 1 & 0 & 0 & \dots \\ 0 & 1 & 0 & \dots \\ 0 & 0 & 1 & \dots \\ \vdots & \vdots & \vdots & \ddots \end{pmatrix}. \tag{4.15}$$

From equation (4.14) we can see that the Green's inverse operator J will have the form

$$J = \begin{pmatrix} 1 & 0 \\ 0 & 1 \end{pmatrix} E - \begin{pmatrix} 1 & 1 \\ -1 & -1 \end{pmatrix} H_0 - \begin{pmatrix} 1 & 0 \\ 0 & -1 \end{pmatrix} mc^2 - \begin{pmatrix} 1 & 0 \\ 0 & 1 \end{pmatrix} V^C \tag{4.16}$$

In the CS basis this takes the form

$$J_{n',n} = \mathbb{1} \cdot E \left\langle n' | n \right\rangle - \begin{pmatrix} 1 & 1 \\ -1 & -1 \end{pmatrix} \left\langle n' \right| H_0 \left| n \right\rangle + \begin{pmatrix} 1 & 0 \\ 0 & -1 \end{pmatrix} mc^2 \left\langle n' | n \right\rangle + \mathbb{1} \cdot Z \delta_{n',n} \tag{4.17}$$

where the CS states are given in from equations (2.6) and (2.7) and $\mathbb{1}$ represents the 2×2 unit matrix. Thus all $J_{n,n'}$ and therefore $G_{n,n'}$ in equation (4.15) are 2×2 block matrices. The 1's and 0's are 2×2 unit and null matrices, respectively.

Due to this structure we can apply the approached used in Ref [12] can calculate the terms of the Green's operator by evaluating the matrix continued fraction defined by

$$(G^N)_{i,j} = (J^N_{i,j} - \delta_{i,N} \delta_{j,N} J_{N,N+1} C_{N+1} J_{N+1,N})^{-1}. \tag{4.18}$$

The numerical evaluation of matrix continued fractions is very similar to those of ordinary continued fractions. Our procedure makes use of backwards evaluation. We start with some $K > N$, which is the value of a higher level basis state and calculate the corresponding 2×2 in the CS basis. We neglect all higher terms and proceed to "roll up" the tail of the continued fraction and evaluate equation (4.18) from the inside out. We are able to choose our level of accuracy but if a new approximant with a larger K is needed, the process starts over again. Though this may be time consuming, depending on the desired level of accuracy, the backwards evaluation is simple and provides very accurate results. We can in essence approximate an entire $\infty \times \infty$ matrix into as small as a 2×2 matrix while still providing extremely accurate results. This continued fraction is convergent for all bound-state energies, giving it considerable advantages over other approximation methods. Furthermore, by using the method presented in [10] it can be continued analytically to the whole complex energy plane. Simple matrix inversion will give the desired Green's matrix.

Our results are in exact agreement with analytic results. Figure 12 shows the exact values of the Klein-Gordon equation for a hydrogen atom in the Coulomb potential as well the convergence of our method. The poles of the Green's matrix occur precisely at the same energy as the analytic bound states. Table 2 displays the exact analytical solution to the Schrödinger equation, followed by the exact analytical solution to the Klein-Gordon equation, and our numerical results using matrix continued fractions, where n is the quantum number. We can see the small effects in the energy due to relativistic considerations. Our procedure results in a 9-digit agreement with analytic results.

TABLE 2. Analytic and numerical Results of a Hydrogen Atom in a Coulomb Potential and Coulomb plus Yukawa potential. n is the principle quantum number.

n	0	1	2	3
Schrödinger (exact)	-0.5000000	-0.1250000	-0.05555555	-0.03125000
KG (exact)	-0.5000332	-0.1250054	-0.05555728	-0.03125075
FV0 Coulomb (numerical)	-0.5000332	- 0.1250054	- 0.05555728	-0.03125075
FV0 Coulomb+Yukawa	-0.3235130	-0.1081552	-0.05119740	-0.03003430

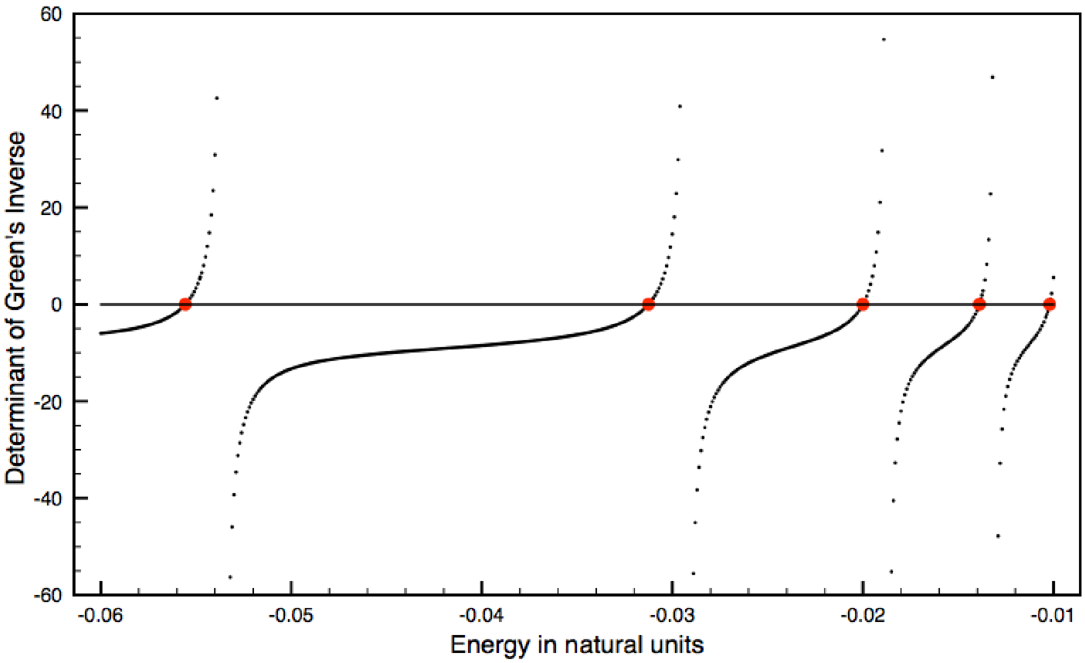

FIGURE 12. Zeroes of the determinant of the Green's inverse matrix and the analytic zeroes of the Klein-Gordon equation. Zeroes of the determinant of the Green's inverse matrix $J = (E - H)$ and the analytic zeroes of the Klein-Gordon equation for the n = 2, 3,4,5,6 states, respectively. The larger dots represent the analytic values.

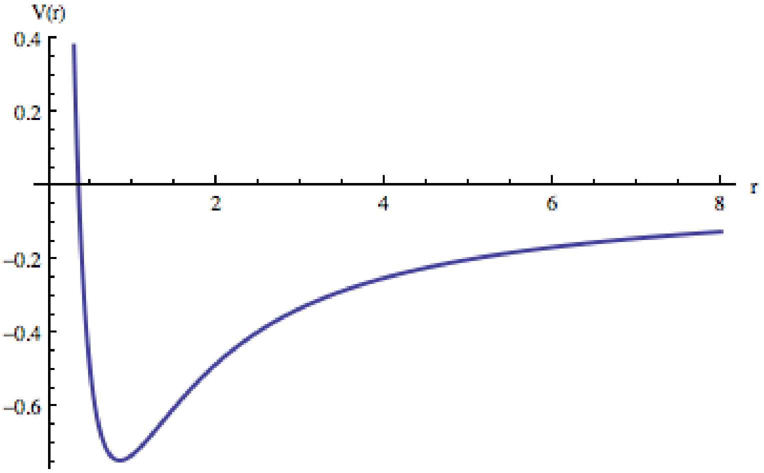

FIGURE 13. Yukawa + Coulomb potential. A Yukawa plus Coulomb potential as given by Eq. (4.20).

In addition to the Coulomb potential, we were able to incorporate a short range potential. By approximating the potential V^s, using the method outlined in chapter 3, and subtracting from the Green's inverse matrix $J = (E - H)$

$$J' = J - V^s, \tag{4.19}$$

the bound state solutions to various short range problems can be obtained.

Yukawa potentials have many applications especially with pions. Our Klein-Gordon equation can describe such a spinless particles. Thus we tested the incorporation of our two techniques by finding the bound states of a particle in a Yukawa potential (see fig. 13):

$$V(r) = \frac{2e^{-2r}}{r}. \tag{4.20}$$

Table 2 has the results of the first few bound states of a hydrogen atom subjected to the Yukawa potential given by (4.20). As expected, this attractive potential raises the ground state energy.

Summary and Conclusion

The goal of our work was to develop a solution method for solving relativistic quantum mechanical equations. The Feshbach-Villars representation of the Klein-Gordon equation has several advantages due to its Hamiltonian form. The FV0 Hamiltonian is a non-hermitian operator and thus violates one of the postulates of QM. Nevertheless, they do produce real eigenvalues and can represent a physical observable. Thus, by relaxing the requirement of hermiticity, the FV0 formalism is able to incorporate relativity into QM.

The price we have to pay is that we have to deal with a two component wave function. The asymptotic coupling by the kinetic energy terms make this Hamiltonian difficult to solve. We overcome this by representing the Green's operator by a matrix continued fraction. Using this procedure we were able to solve for the bound states of the hydrogen-like systems with a 9-digit accuracy. Future advancements would extend this method to include spin and solve the Dirac equation numerically. A part of this work has been published in Ref [9].

BIBLIOGRAPHY

BIBLIOGRAPHY

[1] A. Einstein, *Relativity* (Three Rivers Press, New York, 1961).

[2] N. Zettili, *Quantum Mechanics Concepts and Applications* (John Wiley and Sons, Ltd, New York, 2009).

[3] C. J. R. Serway and C. Moyer, *Modern Physics* (Thomson Learning, Boston, MA, 1989).

[4] R. M. Woodhouse, Ph.D. thesis, California State University, Long Beach, 2012.

[5] A. Wachter, *Relativistic Quantum Mechanics* (Springer, New York, 2011).

[6] M. Srednicki, *Quantum Field Theory* (Cambridge University Press, Cambridge, UK, 2007).

[7] S. K. Kauffmann, arXiv preprint arXiv:1012.5120 (2010).

[8] H. Feshbach and F. Villars, Reviews of Modern Physics **30**, 24 (1958).

[9] N. C. Brown, S. E. Grefe, and Z. Papp, Physical Review C **88**, (2013).

[10] B. Konya, G. Levai, and Z. Papp, Journal of Mathematical Physics **38**, 4832 (1997).

[11] B. Knya and Z. Papp, Journal of Mathematical Physics **40**, (1999).

[12] E. Kelbert *et al.*, Journal of Physics A: Mathematical and Theoretical **40**, 7721 (2007).

[13] F. Demir, Z. T. Hlousek, and Z. Papp, Physical Review A **74**, 014701 (2006).

[14] Z. Papp and W. Plessas, Phys. Rev. C **54**, 50 (1996).

[15] Z. Papp, Phys. Rev. C **55**, 1080 (1997).

[16] Z. Papp, A. Krassnigg, and W. Plessas, Phys. Rev. C **62**, 044004 (2000).

[17] Z. Papp, Phys. Rev. A **46**, 4437 (1992).

[18] S. Adhikari, *Dynamical collision theory and its applications* (Access Online via Elsevier, Waltham, MA, 1991).

[19] J. Revai, JINR E4-9429, Dubna (1975).

[20] B. Gyarmati, A. Kruppa, and J. Revai, Nuclear Physics A **326**, 119 (1979).

[21] S. K. Adhikari and L. Tomio, Phys. Rev. C **36**, 1275 (1987).

[22] J. Darai, B. Gyarmati, B. Kónya, and Z. Papp, Phys. Rev. C **63**, 057001 (2001).